Detections of Screw Penetration during Volar Plating for Distal Radius Fractures

Soo Min Cha, MD, PhD[1] Hyun Dae Shin, MD, PhD[1]

[1] Department of Orthopedic Surgery, Regional Rheumatoid and Degenerative Arthritis Center, Chungnam National University Hospital, Chungnam National University, School of Medicine, Daejeon, Korea

Address for correspondence Hyun Dae Shin, MD, PhD, Department of Orthopedic Surgery, Chungnam National University School of Medicine, 640, Daesa-Dong, Jung-Gu, Daejeon, Korea (e-mail: hyunsd@cnu.ac.kr).

J Wrist Surg 2017;6:340–348.

Abstract

Background We evaluated the detection for screw penetration on the dorsal cortex of the radius in serial oblique, dorsal tangential, and radial groove radiographic views in volar plating fixation.

Materials and Methods Eight screw positions were set in each of the four cadaveric radii. Screw 1 was placed in the styloid subregion, whereas screws 2 and 3 were placed just proximal to the styloid and were defined for the radial region of the radius. Screws 4 (distal to the extensor pollicis longus [EPL] groove), 5 (the distal half of the groove), and 6 (the proximal half of the groove) were placed in the central region of the radius. Screws 7 (just medial to the groove) and 8 (sigmoid notch subregion) were positioned in the ulnar region of the radius. The screws were overlengthened by 1 and 2 mm and were evaluated in three radiographic views.

Results Penetrations in the radial region were fully visible in supinated oblique views with 1- and 2-mm overlengthened screws. The penetration of screw 4 was clearly observable over a considerable range of views. However, the 1-mm penetration of screw 5 was not detectable at any angle of projection. Detection of the ulnar region screw was the most difficult among the three regions with oblique views. In the dorsal tangential view, the 1-mm penetration of screw 4 was not observed in any of the four radii, but the penetration of screw 5 was detectable in all the radii. The screws 2, 3, 5, 7, and 8 were readily detectable. The screw 4 was barely seen in the radial groove view, while the screws 5 and 6 were readily detectable.

Conclusion/Clinical Relevance Appropriate combinations of these well-known radiological views are essential for the overall detection of penetrated screws during plating in distal radius fractures.

Keywords
- screw perforation
- volar plating
- oblique view
- dorsal tangential view
- radial groove view

Complications involving the extensor tendons after volar locking plating in distal radius fractures are well known.[1–3] The incidence of extensor pollicis longus (EPL) rupture after internal fixation of distal radial fractures has been reported to range from 2 to 12.5%.[1,3] Several radiological methodologies have been introduced since the late 2000s to avoid tendon injuries with the penetrating screws. In a previous study, a dorsal horizon view was better at demonstrating protrusion of the screw.[4] The dorsal tangential view was also described with higher sensitivity for detecting the protruded screw.[5] An improved skyline view showed considerable sensitivity and specificity for detecting protrusion through the dorsal cortex by 1 mm.[6,7] The radial groove view has recently been introduced based on an anatomical analysis of

received
December 14, 2016
accepted after revision
May 1, 2017
published online
June 2, 2017

DOI https://doi.org/10.1055/s-0037-1603656.
ISSN 2163-3916.

the third compartment of the extensor surface and has been clinically applied in more than 90 patients; reportedly, any protruding screw in the EPL groove can be detected.[8]

Although perioperative tendon rupture can result from tendon damage caused by a drill bit or from vascular changes resulting from a hematoma, the most common cause of the extensor tendon rupture is screw overlengthening. Several recent reports have described not only "EPL rupture," but also "other extensor injuries."[9–11] These results indicated the need for a thorough intraoperative inspection of penetration of the dorsal cortex of the radius using X-rays.

We hypothesize that an appropriate combination of radiologic methods may be optimal for detecting any penetrated screw among those inserted. In this study, we divided the dorsal cortex of the radius into three regions: (1) radial, (2) central (EPL groove), and (3) ulnar. Then, we evaluated the detection ability of the penetrated screws in the various radiological methods including traditional oblique, dorsal tangential,[5,12] and radial groove views.[8]

Materials and Methods

Cadaver Preparation

This study was approved by our Institutional Review Board (IRB No. CNUH 2014-12-011). We used four radii from four cadavers: two males and two females with a mean age of 64 years. All cadavers were free from any history of trauma in the upper extremity, including bony structures and soft tissues in the record.

Three Regions

After subperiosteal dissection, the dorsal surface was categorized into three regions (radial, central, and ulnar). These

Fig. 1 The three regions and eight subregions of the dorsal radial cortex. (**A**) Each number indicates the location through which each screw would penetrate. Numbers 1, 2, and 3 are in the radial region; 4, 5, and 6 are in the central region; and 7 and 8 are in the ulnar region. (**B**) View from distal to proximal area.

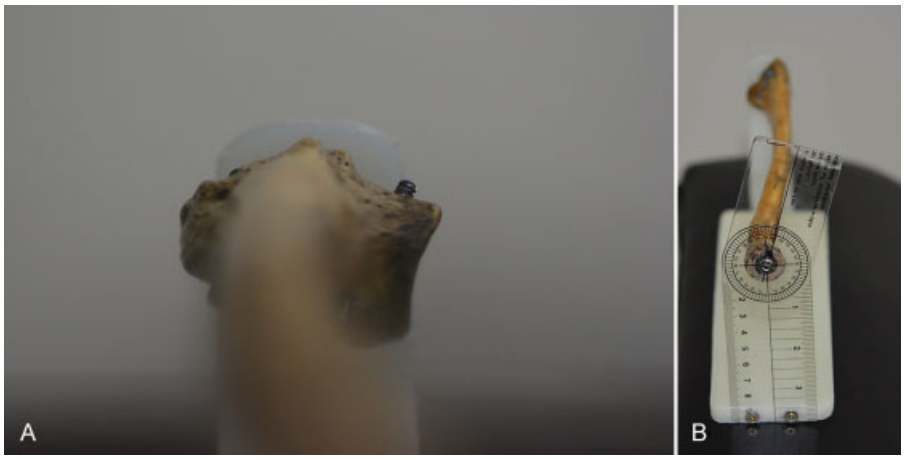

Fig. 2 Figure of jig made for serial oblique views. (**A**) We set the 90-degrees rotation when the Lister's tubercle was in the uppermost position during rotation. (**B**) The center of the rotatory axis was made at the center of the radial head cartilage. A goniometer was used for valid serial rotation. The supination angle was considered positive.

Table 1 Detection of penetrated screws in the radial region under serial angle oblique views

Radial region																			
		Screw 1						Screw 2						Screw 3					
Projection degree		15	20	25	30	35	40	15	20	25	30	35	40	15	20	25	30	35	40
1-mm overlength	Radius 1		V	V	V					V	V						V	V	
	Radius 2		V	V	V	V					V							V	
	Radius 3		V	V	V						V							V	
	Radius 4		V	V	V				V	V	V						V	V	
2-mm overlength	Radius 1	V	V	V	V				V	V	V					V	V	V	
	Radius 2		V	V	V	V			V	V	V					V	V	V	
	Radius 3	V	V	V	V				V	V	V	V				V	V	V	
	Radius 4	V	V	V	V				V	V	V						V	V	V

regions were all defined as the distal region to the proximal margin of the EPL groove. The radial region was considered to be the area lateral to the lateral margin of the EPL groove. The lateral boundary of this area was considered the lateral margin of the groove for the abductor pollicis longus (APL). The central area was defined as the space of the EPL groove and the extension of the space to the distal articular margin. The ulnar area was the medial side, from the medial boundary of the EPL groove (►**Fig. 1**).

Three Subregions

We divided the three regions into two or three subregions in the dorsal surface of the radius. In the radial area, the styloid subregion was designated the distal area from the perpendicular line to the radius axis at the distal margin of the EPL groove. The rest was divided into two subregions, the proximal and distal portions. The central area was surrounded by the dorsal distal edge of the radius (the Lister's tubercle) and the ulnar edge of the EPL groove. The ulnar area was divided into two subregions. One was defined as the more flatter cortex, just medial to the medial margin of the EPL groove; the other was the more protruded portion, comprising the sigmoid notch (►**Fig. 1**).

Overlengthened Screw Insertion

The drill bit was inserted in a retrograde fashion from the dorsal cortex to the volar surface under the fluoroscopic beam at the center of each of the eight subregions. The angle of the drill bit insertion ranged from 45 to 55 degrees in the sagittal plane of the radius. After the eight holes were drilled and the depth of the holes was checked using a depth gauge, 1-mm overlengthened screws were inserted into each of the eight holes from the volar cortex. Then, three different radiological views were taken using a fluoroscope (Siemens AG, Munich, Germany). The same evaluations were repeated with the 2-mm overlengthened screws. Two orthopaedic surgeons identified screws as protruding in each radiological view for every cadaveric radius. The next day, the same two orthopaedic surgeons reevaluated each radiological view, looking for screw protrusion in the same radii. We noted each radiologically protruding screw that was detected unanimously (denoted as V in each table).

Radiological Evaluation

We used three different radiological methods to detect the overlengthening screws on the cortex: traditional oblique, dorsal tangential,[5,12] and radial groove views[8] (►**Supplement Figs.1A** and **1B**, respectively, available in the online version). First, serial projection angles were used for traditional oblique views. To ensure the consistent and valid measurement of serial oblique angles during X-ray projections, we made a jig that rotated the radius with a goniometer. We defined an angle to be 90 degrees when Lister's tubercle was seen most prominently during rotation in the plane parallel to the long axis of the radius. Then, 0-degree angle was indicated in the neutral rotation. Supination angle was considered positive and pronation negative (►**Fig. 2**). The dorsal tangential view was taken with the radius held at 15 degrees dorsally from the vertical axis.[12] Finally, the radial groove view was obtained with a 20-degree upward angle in the horizontal plane and 5 degrees upward in the sagittal plane, as described by Lee et al.[8] The fluoroscopy beam was set perpendicular to the long axis of the radius and jig in the serial oblique views, and vertical to the plane of the ground in the dorsal tangential and radial groove views.

Statistical Analysis

All statistical analyses were done using one-way analysis of variance (ANOVA). Protruding screws were seen at angles of

Table 2 Comparisons of detection of penetrated screws in radial regions under oblique views

Variable	*n*	Mean (SD)	*p*-Value
Screw 1	8	7.87 (1.12)[b]	< 0.01
Screw 2	8	5.43 (2.32)[a,b]	
Screw 3	8	4.88 (1.92)[a]	

Abbreviation: SD, standard deviation.
Note: Scheffe's post hoc test: a $<$ b.

Table 3 Detection of penetrated screws in central region under serial angle oblique views

Central region			Screw 4															Screw 5													Screw 6												
		Projection degree (°)	−45	−40	−35	−30	−25	−20	−15	−10	−5	0	5	10	15	−45	−40	−35	−30	−25	−20	−15	−10	−5	0	5	10	15	−45	−40	−35	−30	−25	−20	−15	−10	−5	0	5	10	15
1-mm overlength	Radius 1		V	V	V	V	V	V	V	V																							V	V	V	V	V	V	V	V	V
	Radius 2		V	V	V	V	V	V	V	V	V																							V	V	V	V	V	V	V	V	V
	Radius 3		V	V	V	V	V	V	V	V																							V	V	V	V	V	V	V	V	V
	Radius 4		V	V	V	V	V	V	V	V	V																							V	V	V	V	V	V	V	V	V
2-mm overlength	Radius 1		V	V	V	V	V	V	V	V	V	V	V	V	V				V	V	V	V	V	V	V	V	V	V				V	V	V	V	V	V	V	V	V	V
	Radius 2		V	V	V	V	V	V	V	V	V	V	V	V	V				V	V	V	V	V	V	V	V	V	V				V	V	V	V	V	V	V	V	V	V
	Radius 3		V	V	V	V	V	V	V	V	V	V	V	V	V				V	V	V	V	V	V	V	V	V	V				V	V	V	V	V	V	V	V	V	V
	Radius 4		V	V	V	V	V	V	V	V	V	V	V	V	V				V	V	V	V	V	V	V	V	V	V				V	V	V	V	V	V	V	V	V	V

15 to 40 degrees (six grades by 5 degrees in radial regions by rotating 5 degrees; ►**Table 1**). Protruding screws in the central regions were seen at angles of 45 to 15 degrees (13 grades by 5 degrees). Thus, we adjusted the grades of detection (V) up to 13, using the weight value concept[13] in the radial and ulnar region analyses. All one-way ANOVA results were also assessed by Scheffe's post hoc test. SPSS (version 19.0) for Windows (SPSS, Inc., Chicago, IL) was used and a p-value < 0.05 was considered statistically significant.

Results

Screw penetration in the radial region was visible in supinated oblique views (range, 15 to 40 degrees; ►**Tables 1** and **2**). Penetration of screw 1 (styloid subregion) was observed to be wider than of the screw 3 ($p < 0.01$). In the central region, penetrating screws were observed from 45 degrees of pronation to approximately15 degrees of supination. Penetration of the screw 4 (juxta-articular subregion distal to the EPL groove) could be clearly observed from 45 degrees of pronation to 15 degrees of supination among the three screws with the 1- and 2-mm overlengths (►**Tables 3** and **4**; $p = 0.03$). The 1-mm penetration was detected from a 45-degree pronation to a 10-degree pronation, and the 2-mm penetration was clearly seen from a 45-degree pronation to a 15-degree supinated view (►**Fig. 3**, ►**Table 3**). Screws within the EPL groove (screws 5 and 6) began to be visible at slightly more supinated views than the screw 4. Penetration of 1 mm and 2 mm in the center of the proximal half of the EPL groove (the screw 6) was seen in a narrower range than the screw 4 (►**Tables 3** and **4**; $p < 0.001$). In addition, 1-mm penetration of screw 5 was not visible at any angle of projection (►**Table 3**). The detection of penetrations in the ulnar region was most difficult among the three regions (all eight screws) in the serial oblique views (►**Tables 5** and **6**; $p < 0.001$). Screws 7 and 8 were just detectable at 30- and 35-degrees pronated oblique views, even with the 2-mm penetrations (►**Table 5**).

Table 4 Comparisons of detection of penetrated screws in central regions under oblique views

Variable	*n*	Mean (SD)	*p*-Value
Screw 4	8 (1 mm and 2 mm)	10.75 (2.43)[b]	0.03
Screw 5		5.38 (5.76)[a]	
Screw 6		7.00 (1.41)[a,b]	
Screw 4	4 (only 1 mm)	8.50 (0.58)[c]	< 0.001
Screw 5		0.00 (0.00)[a]	
Screw 6		5.75 (0.50)[b]	
Screw 4	4 (only 2 mm)	13.00 (0.00)[c]	< 0.001
Screw 5		10.75 (0.50)[b]	
Screw 6		8.25 (0.50)[a]	

Abbreviation: SD, standard deviation.
Note: Scheffe's post hoc test: a < b < c.

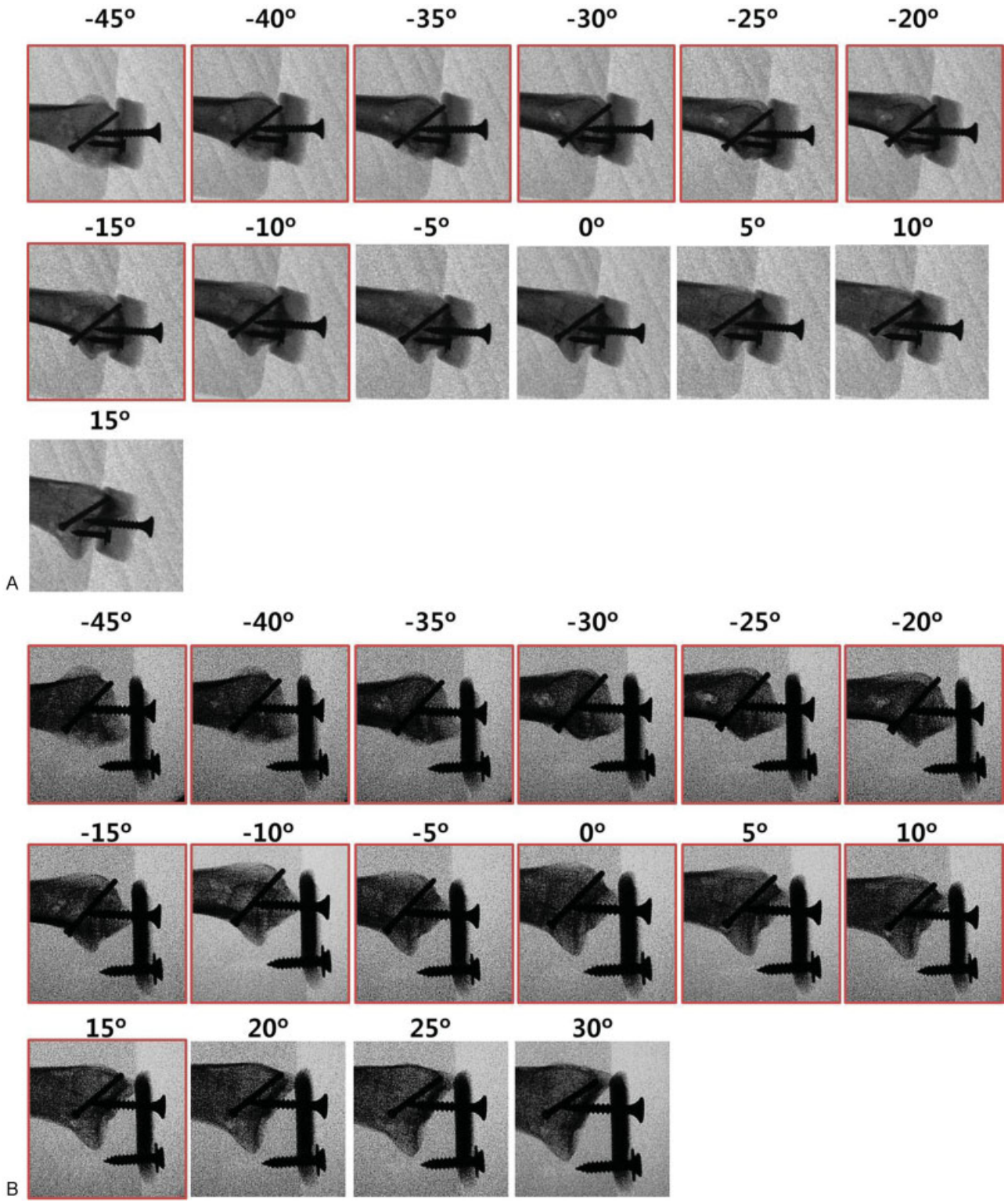

Fig. 3 Detection of screw 4 penetration in radius 1. The red outline indicates detection unanimously four times (two observers × two times each). (**A**) The 1-mm penetrations were seen in 45- to 10-degrees pronated views. (**B**) The 2-mm penetrations were visible in a wider range.

In the dorsal tangential view, 1-mm penetrations of the screws 1 and 6 were relatively difficult to detect, but without statistical significance (►**Tables 7** and **8**). The 1-mm penetration in the juxta-articular subregion distal to the EPL groove (screw 4) was not seen in any of the four cadaveric radii (►**Fig. 4A**). Screws 2, 3, 5, 7, and 8 were readily detectable (►**Tables 7** and **8**).

The radial groove view showed an excellent sensitivity for the detection of penetrations within the EPL groove, such as the screws 5 and 6 (►**Tables 9** and **10**; $p < 0.001$).

Table 5 Detection of penetrated screws in the ulnar region under serial angle oblique views

Ulnar region																	
Screw number		Screw 7							Screw 8								
Projection degree (°)		−45	−40	−35	−30	−25	−20	−15	−10	−5	0	−45	−40	−35	−30	−25	−20	−15	−10	−5	0
1-mm overlength	Radius 1																				
	Radius 2														v						
	Radius 3														v						
	Radius 4																				
2-mm overlength	Radius 1				v									v	v						
	Radius 2			V	v										v						
	Radius 3			V	v									v	v						
	Radius 4				v										v						

Table 6 Overall comparisons of detection of penetrated screws under oblique views

Variable	*n*	Mean (SD)	*p*-Value
Screw 1	8	7.87 (1.12)[b,c]	< 0.001
Screw 2	8	5.43 (2.32)[a,b]	
Screw 3	8	4.88 (1.92)[a,b]	
Screw 4	8	10.75 (2.43)[c]	
Screw 5	8	5.38 (5.76)[a,b]	
Screw 6	8	7.00 (1.41)[b,c]	
Screw 7	8	0.98 (1.15)[a]	
Screw 8	8	1.30 (0.98)[a]	

Abbreviation: SD, standard deviation.
Note: Scheffe's post hoc test: a < b < c.

Table 7 Detection of penetrated screws under a dorsal tangential view

Dorsal tangential view (15 degrees inclination)									
Screw number		1	2	3	4	5	6	7	8
1-mm overlength	Radius 1		V	V		V		V	V
	Radius 2	V		V		V		V	V
	Radius 3			V		V	V	V	V
	Radius 4		V			V		V	V
2-mm overlength	Radius 1	V	V	V		V		V	V
	Radius 2	V	V	V		V	V	V	V
	Radius 3	V	V	V	V	V	V	V	V
	Radius 4	V	V	V		V	V	V	V

Table 8 Comparisons of detection of 1-mm penetrated screws under a dorsal tangential view

Variable	*n*	Mean (SD)	*p*-Value
Screw 1	4	0.25 (0.50)[a,b]	< 0.01
Screw 2	4	0.50 (0.58)[b]	
Screw 3	4	0.75 (0.50)[b,c]	
Screw 4	4	0.00 (0.00)[a]	
Screw 5	4	1.00 (0.00)[c]	
Screw 6	4	0.25 (0.50)[a,b]	
Screw 7	4	1.00 (0.00)[c]	
Screw 8	4	1.00 (0.00)[c]	

Abbreviation: SD, standard deviation.
Note: Scheffe's post hoc test: a < b < c.

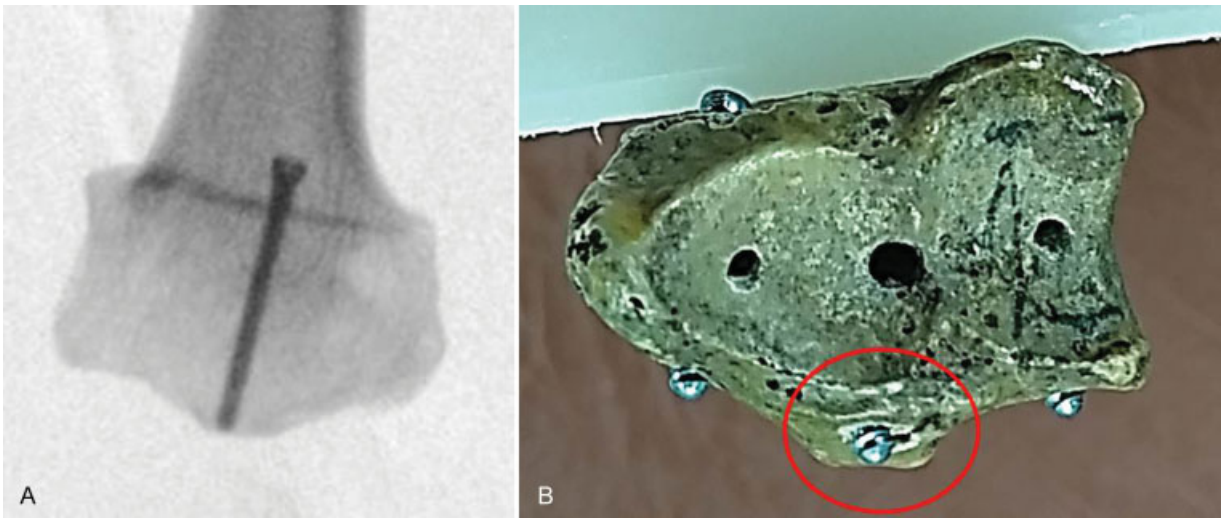

Fig. 4 Dorsal tangential view. (**A**) The 1-mm penetrations of screw 4 were not seen as protruding. (**B**) Penetrated screw located within the proximal bony contour extended from the extensor pollicis longus (EPL) groove. This photograph was taken at the same inclination as the 15-degrees dorsal tangential view.

Table 9 Detection of penetrated screws under a radial groove view

Radial groove view									
Screw number		1	2	3	4	5	6	7	8
1-mm overlength	Radius 1					V	V		
	Radius 2		V			V	V	V	
	Radius 3					V	V		
	Radius 4					V	V	V	
2-mm overlength	Radius 1					V	V	V	V
	Radius 2	V	V		V	V	V	V	V
	Radius 3		V	V		V	V	V	
	Radius 4					V	V	V	V

Penetration in the radial region (screws 1 to 3) was not easily detectable, even with 2-mm overlengthened screws, as they were hidden by Lister's tubercle (►**Fig. 5**; ►**Tables 9** and **10**).

Table 10 Overall comparisons of detection of penetrated screws under a radial groove view

Variable	*n*	Mean (SD)	*p*-Value
Screw 1	8	0.13 (0.35)[a]	< 0.001
Screw 2	8	0.38 (0.52)[a,b]	
Screw 3	8	0.13 (0.35)[a]	
Screw 4	8	0.13 (0.35)[a]	
Screw 5	8	1.00 (0.00)[b]	
Screw 6	8	1.00 (0.00)[b]	
Screw 7	8	0.75 (0.46)[a,b]	
Screw 8	8	0.38 (0.52)[a,b]	

Abbreviation: SD, standard deviation.
Note: Scheffe's post hoc test: a < b.

Discussion

We confirmed that detections for penetrated screws in each region of the dorsal cortex of the distal radius were possible by respective radiological methods through the cadaveric model. Also, overall detections for penetrations on the entire surface of the dorsal cortex more than the EPL groove were sufficiently made by appropriate combinations of radiological methods. We have noted over several years that even the dorsal tangential view at a 15-degree inclination is not suitable for detection just distal to the EPL groove. The newly designed radial groove view by Lee et al[8] was introduced as an effective method based on intraoperative investigation. On the other hand, the screw 4 in our study was not readily detectable even with a 2-mm overlength in the radial groove view. The oblique views (range, 45-degrees pronation to 5-degrees pronation) were more beneficial to assess the penetrated screws in the EPL groove.

The most dorsal prominence of Lister's tubercle prohibited radiological viewing at a tangential view, and an upward projection angle of 5 degrees in the sagittal plane (radial

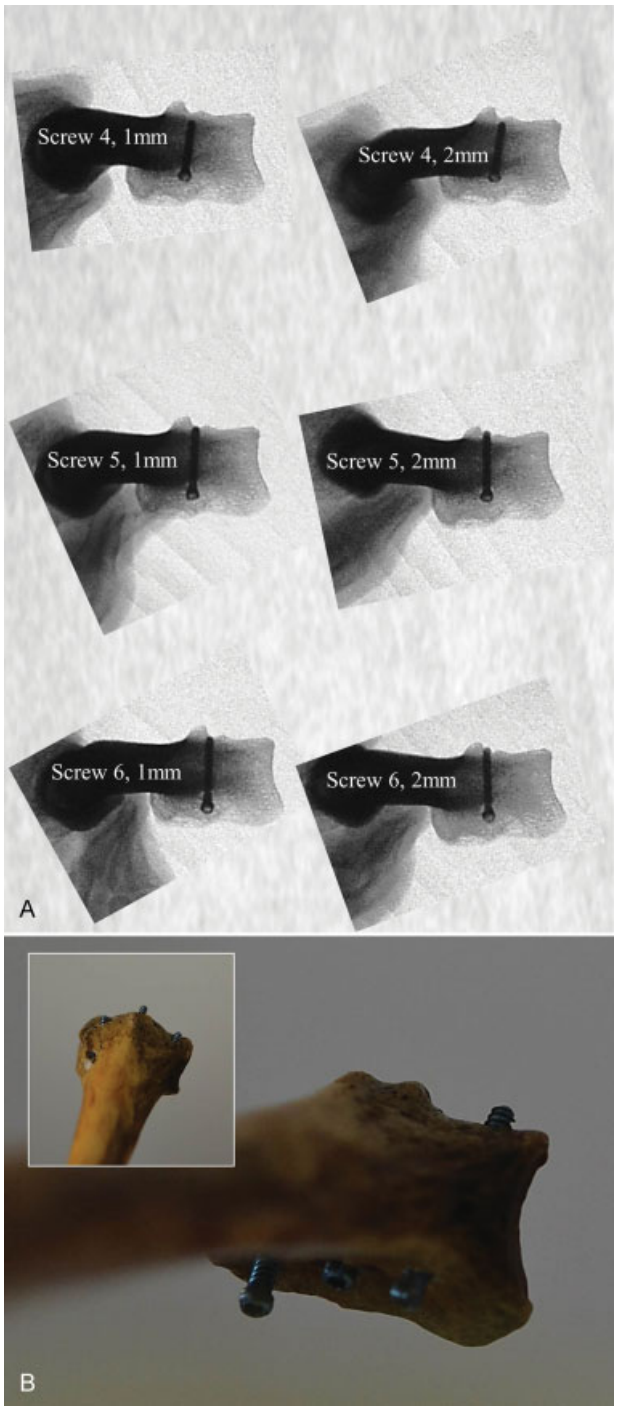

Fig. 5 Radial groove view. (**A**) Even the 2-mm penetration of screw 4 in radius 3 was not detectable as protruding. However, 1-mm penetrations of screws 5 and 6 were easily detected. (**B**) Concurrent 2-mm penetrations of screws 2, 4, and 8 in radius 4 were observed at the same angle as the radial groove view, but only screw 8 was seen.

groove view) did not show the penetrated screw at more distal surfaces (►**Figs. 4B** and **5B**). The screw 5 (distal EPL groove) was most visible in tangential and radial groove views to similar degrees. The location of the screw 5 was considered to be the same as the screws protruding in the EPL groove in other reports. The more proximal screw in the EPL groove (the screw 6) was less sensitive in the tangential view than in the pronated oblique views due to the decreased depth of the EPL groove. Penetrating screws in the ulnar area (screws 7, 8) were not seen due to the anatomical features of the ulnar side slope of the EPL groove/flat area/sigmoid notch prominence in pronated views. However, a tangential view is strongly recommended for these screws, consistent with previous studies that investigated the dorsal tangential/skyline view.[4,5,7,12,14–17] The differences between the current study and a previous study of the dorsal tangential view[5] are that we compared the efficacy of the more recently developed radial groove view and tangential views. Based on our study, screw penetration through the proximal half of the EPL groove was more easily detectable using the radial groove view. We also emphasized the "juxta-articular location" just distal to the EPL groove, in which screw penetration was not seen easily with either the dorsal tangential or radial groove view.

A limitation of our study was that the validity of the consecutive angles of the oblique views under intraoperative conditions was unclear. We set the angles on our own jig using Lister's tubercle as a landmark, but with the use of an image intensifier during the operation, it was not easy to measure precise beam projection angles during forearm rotation. However, the range of visible angles and specific angles of detection on the jig were good indicators of the presence of screw penetration for "real-time" imaging around the suggested angles during an operation for each screw. In addition, our results were gained from nonfractured human radii. Under clinical conditions, fractures with an intact dorsal cortex are at a lower risk for dorsal penetration compared with fractures with a comminuted dorsal cortex. Thus, our suggestions may not be completely applicable to radial fractures with dorsal cortex comminution with the possibility of invisible screw penetration between the fragments.

We conclude that appropriate combinations of radiological views are beneficial for the detection of penetrated screws. Especially, the presence of a protruding screw in the juxta-articular area just distal to the EPL groove should not be missed. Screw penetration in this area was readily seen in serial oblique views better than in the specific views of the EPL groove. Finally, the radial groove view appears to be more useful than the dorsal tangential view for the detection of penetrated screws in the proximal half of EPL groove.

Ethical Review Committee Statement
Our Institutional Review Board approved this study (IRB No. CNUH 2014–12–011).

Funding
None.

Conflict of Interest
None.

Acknowledgments
The authors thank Kyung Bo Seo, PhD (Expectblue Company, Seoul, Korea) for assistance with the statistical analysis.

References

1 Arora R, Lutz M, Hennerbichler A, Krappinger D, Espen D, Gabl M. Complications following internal fixation of unstable distal radius fracture with a palmar locking-plate. J Orthop Trauma 2007; 21(05):316–322

2 Benson EC, DeCarvalho A, Mikola EA, Veitch JM, Moneim MS. Two potential causes of EPL rupture after distal radius volar plate fixation. Clin Orthop Relat Res 2006;451:218–222

3 Bianchi S, van Aaken J, Glauser T, Martinoli C, Beaulieu JY, Della Santa D. Screw impingement on the extensor tendons in distal radius fractures treated by volar plating: sonographic appearance. Am J Roentgenol 2008;191(05):W199–W203

4 Joseph SJ, Harvey JN. The dorsal horizon view: detecting screw protrusion at the distal radius. J Hand Surg Am 2011;36(10): 1691–1693

5 Ozer K, Wolf JM, Watkins B, Hak DJ. Comparison of 4 fluoroscopic views for dorsal cortex screw penetration after volar plating of the distal radius. J Hand Surg Am 2012;37(05): 963–967

6 Pichler W, Windisch G, Schaffler G, Rienmüller R, Grechenig W. Computer tomography aided 3D analysis of the distal dorsal radius surface and the effects on volar plate osteosynthesis. J Hand Surg Eur Vol 2009;34(05):598–602

7 Riddick AP, Hickey B, White SP. Accuracy of the skyline view for detecting dorsal cortical penetration during volar distal radius fixation. J Hand Surg Eur Vol 2012;37(05):407–411

8 Lee SK, Bae KW, Choy WS. Use of the radial groove view intra-operatively to prevent damage to the extensor pollicis longus tendon by protruding screws during volar plating of a distal radial fracture. Bone Joint J 2013;95-B(10):1372–1376

9 Hattori Y, Doi K, Sakamoto S, Yukata K. Delayed rupture of extensor digitorum communis tendon following volar plating of distal radius fracture. Hand Surg 2008;13(03):183–185

10 Ward JP, Kim LT, Rettig ME. Extensor indicis proprius and extensor digitorum communis rupture after volar locked plating of the distal radius–a case report. Bull NYU Hosp Jt Dis 2012;70(04):273–275

11 Singh HP, Srinivasan S, Ullah A. Closed rupture of the extensor indicis and extensor digitorum tendons to the index finger after locking plate fixation of a fracture of the distal radius. J Hand Surg Eur Vol 2013;38(01):86–87

12 Haug LC, Glodny B, Deml C, Lutz M, Attal R. A new radiological method to detect dorsally penetrating screws when using volar locking plates in distal radial fractures. The dorsal horizon view. Bone Joint J 2013;95-B(08):1101–1105

13 Liou T-S, Wang M-JJ. Ranking fuzzy numbers with integral value. J Statistical Field 1992;50(03):247–255

14 Brunner A, Siebert C, Stieger C, Kastius A, Link BC, Babst R. The dorsal tangential X-ray view to determine dorsal screw penetration during volar plating of distal radius fractures. J Hand Surg Am 2015;40(01):27–33

15 Clement H, Pichler W, Nelson D, Hausleitner L, Tesch NP, Grechenig W. Morphometric analysis of Lister's tubercle and its consequences on volar plate fixation of distal radius fractures. J Hand Surg Am 2008;33(10):1716–1719

16 Knight D, Hajducka C, Will E, McQueen M. Locked volar plating for unstable distal radial fractures: clinical and radiological outcomes. Injury 2010;41(02):184–189

17 Maschke SD, Evans PJ, Schub D, Drake R, Lawton JN. Radiographic evaluation of dorsal screw penetration after volar fixed-angle plating of the distal radius: a cadaveric study. Hand (NY) 2007; 2(03):144–150